Reactions of Laser-Ablated Gold with Nitric Oxide: Infrared Spectra and DFT Calculations of AuNO and $Au(NO)_2$ in Solid Argon and Neon†

Angelo Citra, Xuefeng Wang, and Lester Andrews*

Department of Chemistry, University of Virginia, Charlottesville, Virginia 22904-4319

Received: March 9, 2001; In Final Form: May 25, 2001

Laser-ablated gold reacts with nitric oxide in excess argon and neon, yielding the neutral nitrosyl complexes AuNO and $Au(NO)_2$ as the main products. The N−O and Au−N stretching modes of AuNO are observed at 1701.9 and 517.6 cm^{-1} in solid argon and at 1710.4 and 523.8 cm^{-1} in solid neon. Both BPW91 and B3LYP density functionals predict $^1A'$ state frequencies in very good agreement. An NBO analysis suggests more d orbital involvement in the bonding in AuNO than in the copper and silver nitrosyls. The dinitrosyl $Au(NO)_2$ is observed at 1510.7 and 3183.2 cm^{-1} in solid argon and at 1528.2 and 3204.1 cm^{-1} in solid neon, which are in good agreement with DFT quartet state fundamental and combination frequencies: $Au(NO)_2$ shows evidence for increased charge transfer and sd hybridization compared to AuNO. The cation nitrosyls $Au(NO)_{1,2}^+$ are minor products.

Introduction

Although gold is well-known for its inertness as a precious metal, it does exhibit some catalytic activity. For example gold supported on silica and alumina catalyzes the reduction of NO with H_2.[1] Furthermore, nitric oxide adsorbed on gold-impregnated NaY zeolite catalysts shows infrared absorptions at 1880 and 1910 cm^{-1}, respectively, which have been identified as mononitrosyl species.[2] Similar results are observed for nitric oxide on Au(I)/ZSM-5 zeolite, and additional bands at 1837 and 1741 cm^{-1} are attributed to $Au^I(NO)_2$.[3] Matrix isolation spectra of AuNO and $Au(NO)_2$ will provide a benchmark for comparison of the adsorbed NO species as found in recent investigations of copper and silver nitrosyls.[4,5]

In this work laser-ablated gold is reacted with nitric oxide, and the products are isolated in solid argon and neon and characterized using infrared spectroscopy and density functional theory (DFT) calculations. The observed products show similarities with both the copper and silver nitrosyls,[4,5] but also marked differences, which are of interest to understand the bonding in noble metal compounds. An NBO analysis of the bonding in Cu, Ag, and Au nitrosyls finds more d-orbital involvement with gold.

Experimental and Theoretical Methods

The experiment for laser ablation and matrix isolation has been described in detail previously.[6] Briefly, the Nd:YAG laser fundamental (1064 nm, 10 Hz repetition rate, 10 ns pulse width, 5−50 mJ/pulse) was focused on a rotating gold metal target. Laser-ablated metal atoms, cations and electrons were codeposited with nitric oxide at 0.6−0.1% in argon or 1%-0.04% in neon onto a 7−8 or 4−5 K CsI window at 2−4 mmol/h for 2 h or 30 min. Several isotopic samples ($^{14}N^{16}O$, Matheson; $^{15}N^{16}O$, MDS isotopes, 99%; $^{15}N^{18}O$, Isotec, 99%) and selected mixtures were used. Infrared spectra were recorded at 0.5 cm^{-1} resolution on a Nicolet 750 spectrometer with 0.1 cm^{-1} accuracy using a HgCdTe detector. Matrix samples were annealed at a range of temperatures (20−45 K, argon; 6−12 K, neon) and subjected to broad-band photolysis by a medium-pressure mercury arc (Philips, 175 W) with the globe removed ($\lambda > 240$ nm).

Density functional theory (DFT) calculations were performed on gold nitrosyls using the Gaussian 94 program.[7] The BPW91 functional was used in all calculations, with the B3LYP functional employed for comparison in selected cases.[8−10] The 6-311+G(d) basis set was used to represent nitrogen and oxygen,[11] and the LanL2DZ ECP basis set was used for gold.[12]

Results

Absorptions for gold nitrosyl products in pure and mixed isotopic experiments in solid argon and neon are listed in Tables 1 and 2. Additional bands due to NO, $(NO)_2$, $(NO)_2^+$, $(NO)_2^-$, NO_2, NO_2^-, $(NO)_3^-$, and N_2O_3 common to experiments with laser-ablated metal and nitric oxide are not listed in the tables.[13−16] Figures 1 and 2 illustrate the spectra of Au and NO samples codeposited in argon at 8−9 K, and Figures 3 and 4 show spectra in solid neon at 4−5 K. Figure 5 contrasts spectra in the 1900 cm^{-1} region with CCl_4 added to enhance the cation yield. Optimized geometries and harmonic frequencies of anticipated product molecules calculated using DFT are summarized in Tables 3 and 4, force constants calculated for AuNO are given in Table 5, and the computed atomic charges are listed in Table 6.

Discussion

Gold nitrosyl products in solid argon and neon will be identified from isotopic substitution and DFT frequency calculations.

AuNO. An intense band observed at 1701.9 cm^{-1} after deposition in argon grows slightly during early annealing (Figure 1). The $^{15}N^{16}O$ and $^{15}N^{18}O$ counterparts at 1672.4 and 1626.8 cm^{-1} give $^{14}N^{16}O/^{15}N^{16}O$ and $^{15}N^{16}O/^{15}N^{18}O$ ratios of 1.0176 and 1.0280, respectively. These are virtually identical to the frequency ratios 1.0176 and 1.0277 for isolated NO,[14] which indicates that there is essentially no coupling between the Au−N

† Part of the special issue "Mitsuo Tasumi Festschrift".

10.1021/jp010911a CCC: $22.00
Published on Web 07/24/2001

TABLE 1: Infrared Absorptions (cm^{-1}) Observed for Gold and Nitric Oxide in Argon at 7−8 K

$^{14}N^{16}O$	$^{15}N^{16}O$ [$^{14}N^{16}O/^{15}N^{16}O$]	$^{15}N^{18}O$ [$^{15}N^{16}O/^{15}N^{18}O$]	$^{14}N^{16}O + {}^{15}N^{16}O$	$^{15}N^{16}O + {}^{15}N^{18}O$	assignment
3372.5	3314.7 [1.0174]	3224.9 [1.0278]	3372.5, 3314.7	3314.7, 3224.9	AuNO, 2ν
3183.2	3126.7 [1.0181]				$Au(NO)_2$
3173.2	3116.8 [1.0181]				$Au(NO)_2$ (site)
1846.8	1814.2 [1.0180]	1765.6 [1.0275]	1814.2	1765.6	Au_x-$(NO)_2$ (site)
1843.8	1811.4 [1.0179]	1762.6 [1.0277]	1811.4	1762.6	Au_x-$(NO)_2$
1759.7	1729.0 [1.0178]	1682.2 [1.0278]	1759.7, 1737.8, 1729.0	1682.2	Au_x-$(NO)_2$ (site)
1754.5	1723.8 [1.0178]	1677.1 [1.0278]	1754.5, 1733.2, 1723.8	1723.8, 1686.2, 1677.1	$Au(NO)_2$
1701.9	1672.4 [1.0176]	1626.8 [1.0280]	1701.9, 1672.4	1672.4, 1626.8	AuNO
1699.6	1670.1 [1.0177]	1624.7 [1.0279]	1699.6, 1670.1	1670.1, 1624.7	AuNO (site)
1671.4	1641.8 [1.0180]	1597.6 [1.0277]			Au_xNO
1538.2	1510.7 [1.0182]	1471.4 [1.0267]	1538.2, 1526.8, 1519.4, 1510.7	1538.2, 1493.4, 1471.4	Au(NO)(NO)′
1511.8	1484.7 [1.0183]	1446.4 [1.0265]	1511.8, 1497.2, 1484.7	1484.7, 1463.2, 1446.4	$Au(NO)_2$ (site)
1510.7	1483.5 [1.0183]	1445.3 [1.0264]	1510.7, 1496.0, 1483.5	1483.5, 1462.3, 1445.3	$Au(NO)_2$
1509.5	1482.3 [1.0183]	1444.1 [1.0265]	1509.5, 1494.9, 1482.3	1482.3, 1461.2, 1444.1	$Au(NO)_2$ (site)
1507.9	1481.1 [1.0181]	1442.3 [1.0269]	1507.9, 1493.2 1481.1	1481.1, 1459.3, 1442.3	$Au(NO)_2$ (site)
518.6	505.1 [1.0267]	499.6 [1.0110]			AuNO (site)
517.6	504.1 [1.0268]	498.6 [1.0110]	517.8, 504.0	504.0, 498.5	AuNO

TABLE 2: Infrared Absorptions (cm^{-1}) Observed for Gold and Nitric Oxide in Neon at 4−5 K

$^{14}N^{16}O$	$^{15}N^{16}O$ [$^{14}N^{16}O/^{15}N^{16}O$]	$^{15}N^{18}O$ [$^{15}N^{16}O/^{15}N^{18}O$]	$^{14}N^{16}O + {}^{15}N^{16}O$	$^{15}N^{16}O + {}^{15}N^{18}O$	assignment
3388.8	3330.9 [1.0174]	3241.4 [1.0276]	3388.8, 3330.9		AuNO, 2ν
3212.6	3155.5 [1.0181]	3074.2 [1.0264]	3212.6, 3185.1, 3155.5		$Au(NO)_2$ (trans)
3204.1	3147.1 [1.0181]	3066.0 [1.0264]	3204.1, 3176.5, 3147.1		$Au(NO)_2$ (cis)
1921.2	1887.3 [1.0180]				$AuNO^+$ (site)
1917.8	1883.9 [1.0180]				$AuNO^+$
1899.4	1865.8 [1.0180]				$Au(NO)_2^+$ (site)
1895.7	1862.2 [1.0180]				$Au(NO)_2^+$
1892.0	1858.6 [1.0180]				$Au(NO)_2^+$ (site)
1718.1	1688.5 [1.0175]	1642.6 [1.0279]	1718.1, 1688.5	1688.5, 1642.6	AuNO (site)
1710.4	1681.2 [1.0174]	1635.3 [1.0281]	1710.4, 1681.2	1681.2, 1635.3	AuNO
1709.4	1680.0 [1.0175]	1634.0 [1.0282]	1709.4, 1680.0	1680.0, 1634.0	AuNO (site)
1556.5	1528.4 [1.0184]	1488.9 [1.0265]	1556.5, 1545.8	1528.4, 1488.9	Au(NO)(NO)′
1532.9	1505.2 [1.0184]	1466.3 [1.0265]	1532.9, 1517.8, 1505.2	1505.2,1481.3, 1466.3	$Au(NO)_2$ (trans)
1530.2	1503.1 [1.0180]	1464.2 [1.0266]	1530.2, 1515.8, 1503.1	1503.1, 1479.6, 1464.2	$Au(NO)_2$ (site)
1528.2	1500.5 [1.0184]	1461.7 [1.0265]	1528.1, 1513.1, 1500.5	1500.5, 1478.4, 1461.7	$Au(NO)_2$ (cis)
527.2	513.2 [1.0273]		527.2, 513.2		AuNO (site)
523.8	509.7 [1.0277]		523.8, 509.7		AuNO

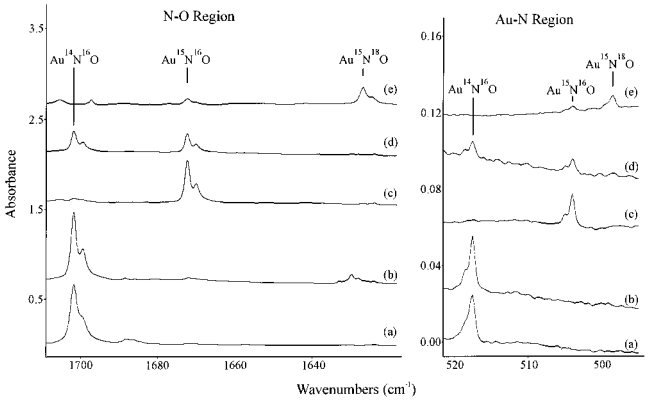

Figure 1. Infrared spectra in the 1710−1610 and 520−490 cm^{-1} regions for laser-ablated gold and NO after (a) 60 min deposition with 0.3% $^{14}N^{16}O$ in argon, (b) annealing to 25 K, (c) 60 min deposition with 0.2% $^{15}N^{16}O$ in argon and annealing to 25 K, (d) 60 min deposition with 0.15% $^{14}N^{16}O$ and 0.15% $^{15}N^{16}O$ in argon and annealing to 25 K, and (e) 60 min deposition with 0.3% $^{15}N^{18}O$ and 0.1% $^{15}N^{16}O$ in argon, and annealing to 25 K.

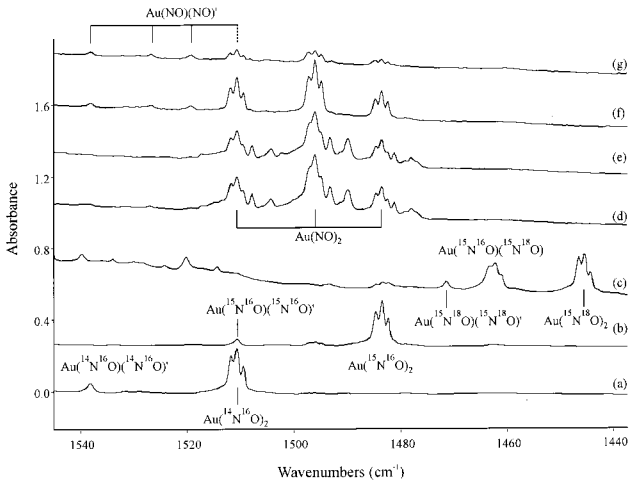

Figure 2. Infrared spectra in the 1540−1440 cm^{-1} region for laser-ablated gold and NO after (a) 60 min deposition with 0.3% NO in argon and annealing to 35 K, (b) 60 min deposition with 0.2% ^{15}NO in argon and annealing to 35 K, (c) 60 min deposition with 0.3% $^{15}N^{18}O$ and 0.1% ^{15}NO in argon and annealing to 35 K, (d) 60 min deposition with 0.15% NO and 0.15% ^{15}NO in argon and annealing to 25 K, (e) 25 min irradiation, (f) annealing to 35 K, and (g) annealing to 40 K.

and N−O stretching modes. Only the 1701.9, 1672.4, and 1626.8 cm^{-1} bands are observed in the $^{14}N^{16}O + {}^{15}N^{16}O$ and $^{15}N^{16}O + {}^{15}N^{18}O$ mixed isotope experiments, showing that only one NO molecule is involved in this vibrational mode. The bands are therefore assigned to the mononitrosyl AuNO. The isotopic ratios are similar to CuNO and AgNO but very different from those for other MNO molecules observed in this laboratory, which commonly have $^{14}N^{16}O/^{15}N^{16}O$ ratios between 1.0194 and 1.0225 and thus exhibit more mode mixing.[17−25] The neon matrix counterpart at 1710.4 cm^{-1} (Figure 3) exhibits the small blue shift relative to argon typical for these molecules, as does NO from 1871.8 cm^{-1} in solid argon to 1874.4 cm^{-1} in solid neon,[15] which are just below the 1876.1 cm^{-1} gas-phase value.[26]

The overtone of the N−O fundamental in AuNO was observed at 3372.5 and 3388.8 cm^{-1} in solid argon and neon,

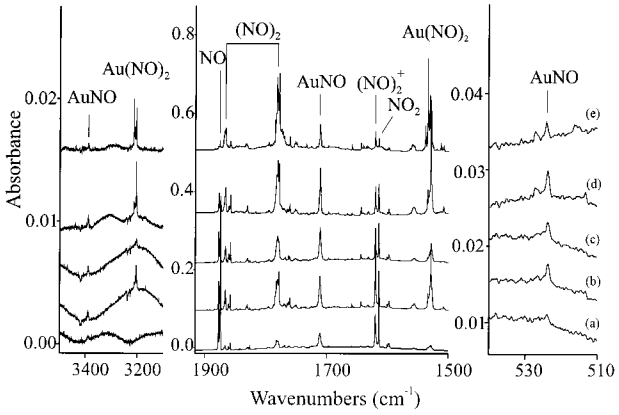

Figure 3. Infrared spectra in the 3500−3100, 1950−1500, and 540−510 cm^{-1} regions for laser-ablated gold and NO after (a) 30 min deposition with 0.2% NO in neon, (b) annealing to 9 K, (c) $\lambda > 370$ nm irradiation, (d) annealing to 11 K, and (e) annealing to 13 K.

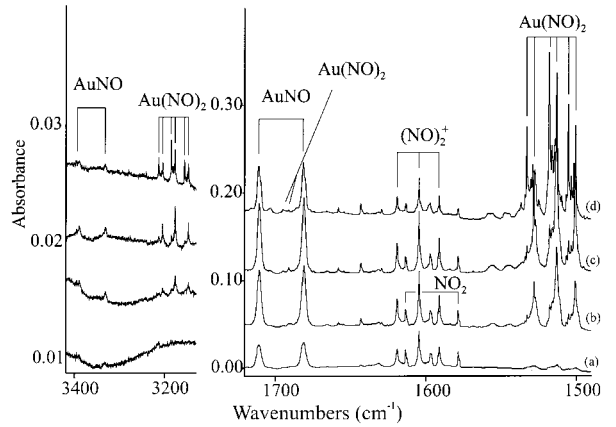

Figure 4. Infrared spectra in the 3410−3130 and 1720−1490 cm^{-1} regions for laser-ablated gold and NO after (a) 30 min deposition of 0.1% ^{14}NO and 0.1% ^{15}NO in neon, (b) annealing to 9 K, (c) annealing to 11 K, and (d) annealing to 13 K.

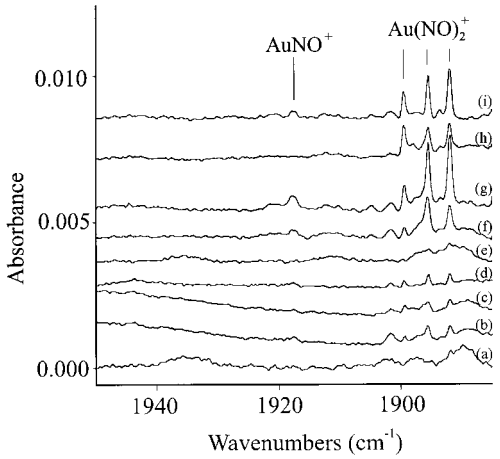

Figure 5. Infrared spectra in the 1950−1885 cm^{-1} region for laser-ablated gold and NO after (a) 30 min deposition with 0.2% NO in neon, (b) annealing to 9 K, (c) $\lambda > 240$ nm irradiation, (d) annealing to 11 K, (e) 30 min deposition with 0.2% NO and 0.02% CCl_4 in neon, (f) annealing to 9 K, (g) annealing to 11 K, (h) $\lambda > 240$ nm irradiation, and (i) annealing to 12 K.

respectively, which are 31.3 and 32.0 cm^{-1} lower than double the fundamental frequencies. This is reasonable for normal cubic anharmonicity, which is essentially the same in solid argon and neon.

Another band observed at 517.6 cm^{-1} tracks with the 1701.9 cm^{-1} absorption in argon and has only 1/27 of the intensity of the higher frequency absorption. The band forms a 1:1 doublet at 517.6 and 504.1 cm^{-1} in the $^{14}NO + {}^{15}NO$ experiment. The $^{14}N^{16}O/^{15}N^{16}O$ and $^{15}N^{16}O/^{15}N^{18}O$ isotopic frequency ratios for this band are 1.0268 and 1.0110, respectively. The former ratio approaches the harmonic diatomic ratio of 1.0326 for AuN, and the band is therefore assigned to the Au−N stretching mode in AuNO. The isotopic data for these bands provides enough information to estimate the force constants and bond angle, and the results of this calculation are summarized in Table 5. The parameters included in this calculation to fit isotopic frequencies are the Au−N and N−O stretching force constants, the sretch−stretch interaction constant, and the bond angle. No experimental data are available for the bending mode, which is ignored. The isotopic data provided nine sets of values for these parameters. The uncertainties in the force constants are large, but this approximate vibrational analysis shows that the bond angle is clearly much less than 180°. The neon matrix counterpart at 523.8 cm^{-1} again exhibits a small blue shift, which characterizes a relatively minor matrix interaction for AuNO.

The DFT calculations for AuNO are in very good agreement with experiment. The $^1A'$ state is calculated to be considerably lower in energy than the $^3A''$ state with both the BPW91 (Table 3) and B3LYP (Table 4) functionals. In addition, the computed N−O frequencies are higher for the $^1A'$ state than observed and lower for the $^3A''$ state, which suggests the former as the ground state. The Au−N stretching frequencies of 339.9 cm^{-1} (BPW91) and 278.0 cm^{-1} (B3LYP) calculated for the $^3A''$ state are much lower than the 517.6 cm^{-1} experimental value, but the $^1A'$ state predictions 526.0 cm^{-1} (BPW91) and 521.6 cm^{-1} (B3LYP) are in agreement. The $^1A'$ state is therefore identified as the ground state for AuNO. The NO stretching frequency of 1764.3 cm^{-1} calculated with BPW91 is 62.4 cm^{-1} higher than the argon matrix experimental value, in slightly greater error than analogous calculations for the group VIII metal nitrosyls,[17−19] but comparable with the accuracy for copper and silver nitrosyls.[4,5] The isotopic frequency ratios for this mode are calculated to be 1.0179 and 1.0286 with both functionals, in excellent agreement with the experimental values of 1.0179 and 1.0277. The predominantly Au−N stretching mode is calculated within 10 cm^{-1} of the observed value in each case. The $^{14}N^{16}O/^{15}N^{16}O$ and $^{15}N^{16}O/^{15}N^{18}O$ isotopic ratios of 1.0277 and 1.0109 (BPW91) and 1.0272 and 1.0120 (B3LYP) are also in very good agreement with experiment, as are the calculated intensity ratios of 49:1 (BPW91) and 57:1 (B3LYP) for the two stretching modes. Finally, the nonlinear geometry calculated for AuNO is in qualitative agreement with the approximate bond angle determination from the argon matrix isotopic frequencies.

DFT calculations were done for dimers of AuNO. The C_{2h} structure observed for $Ag(NO)_2Ag$ revealed a strong N−O fundamental at 1185.5 cm^{-1}, and the D_{2h} isomer found for $Cu_2(NO)_2$ had a very strong 1499.6 cm^{-1} absorption.[4,5] These structures are higher in energy than two AuNO molecules. The only $Au_2N_2O_2$ isomer computed to be lower was an asymmetric species with strong 1667 and 1541 cm^{-1} absorptions, which were not observed in the spectrum.

$Au(NO)_2$. The 1510.7 cm^{-1} band and associated matrix site absorptions are weak on deposition but increase markedly on annealing and decrease on photolysis. Isotopic and mixed isotopic spectra are shown in Figure 2: the 1:2:1 triplet pattern for the $^{14}NO + {}^{15}NO$ spectrum indicates that two equivalent NO subunits are involved in the vibration. The neon matrix counterpart at 1528.2 cm^{-1} behaves similarly: the parallel annealing and photolysis behavior, as well as matrix site

TABLE 3: Geometries, Energies, and Frequencies Calculated for Neutral and Ionic Gold Nitrosyls Using DFT (BPW91/LanL2DZ/6-311+G(d))

molecule	state (point group)	rel energies (kJ/mol)	$\langle S^2 \rangle$	geometry (Å, deg)	frequencies (cm^{-1}) [intensities (km/mol)]
AuNO	$^1A'$ (C_s)	0		AuN: 2.094 NO: 1.161 ∠AuNO: 118.8	1764.3 [828], 526.0 [17], 261.1 [6]
	$^3A''$ (C_s)	+79	2.0000	AuN: 2.101 NO: 1.190 ∠AuNO: 127.6	1656.3 [564], 339.9 [2], 199.3 [4]
$AuNO^+$	$^2A'$ (C_s)	+859	0.7500	AuN: 2.112 NO: 1.130 ∠AuNO: 125.8	1935.4 [668], 365.9 [15], 214.5 [19]
$Au(NO)_2$	$^2B_1$ (C_{2v})	0	0.7500	AuN: 2.058 NO: 1.177 ∠AuNO: 127.0 ∠NAuN: 165.1	1735.4 [83], 1657.8 [2301], 459.1 [1], 446.9 [19], ..., 70.5 [0]
	^4B_g (C_{2h})	+34	3.7500	AuN: 2.001 NO: 1.191 ∠AuNO: 134.5 ∠NAuN: 180.0	1704.8 [0], 1616.7 [1983], 461.4 [1], 388.3 [0], ..., 60.7 [0.4]
	$^4A_2$ (C_{2v})	+39	3.7500	AuN: 2.009 NO: 1.192 ∠AuNO: 131.9 ∠NAuN: 172.9	1699.3 [6], 1604.7 [1964], 418.9 [1], 402.8 [1], ..., 70.5 [0]
$Au(NO)_2^+$	$^1A_1$ (C_{2v})	+773		AuN: 2.222 NO: 1.131 ∠AuNO: 121.9 ∠NAuN: 125.5	1951.1 [378], 1905.7 [1290], 501.0 [23], 387.9 [1], ..., −44.8 [0.3]
$Au(NO)_3$	$^5A''$ (C_s)	0	6.0000	AuN: 2.009, 2.310, 2.310 NO: 1.194, 2.310, 2.310 ∠AuNO: 132.7, 122.7, 122.7 ∠NAuN: 149.4, 61.0, 61.0	1748.6 [285], 1619.8 [1726], 1609.8 [904], ... −87.2 [1]

TABLE 4: Geometries, Energies, and Frequencies Calculated for Selected Neutral and Ionic Gold Nitrosyls Using DFT (B3LYP/LanL2DZ/6-311+G(d))

molecule	state (point group)	rel energies (kJ/mol)	$\langle S^2 \rangle$	geometry (Å, deg)	frequencies (cm^{-1}) [intensities (km/mol)]
AuNO	$^1A'$ (C_s)			AuN: 2.115 NO: 1.149 ∠AuNO: 118.2	1824.2 [1132], 521.6 [20], 254.4 [7]
	$3A''$ (C_s)	+50	2.0000	AuN: 2.198 NO: 1.173 ∠AuNO: 125.7	1740.2 [821], 278.0 [3], 155.6 [9]
$AuNO^+$	$^2A'$ (C_s)	+840	0.7500	AuN: 2.189 NO: 1.118 ∠AuNO: 125.3	2015.4 [869], 338.4 [14], 180.8 [15]
$Au(NO)_2$	^4B_g (C_{2h})	0	3.7502	AuN: 1.998 NO: 1.180 ∠AuNO: 134.8 ∠NAuN: 180.0	1782.1 [0], 1598.2 [4700], 478.1 [5], 403.2 [0], ..., 59.9 [0]
	$^4A_2$ (C_{2v})	+5	3.7502	AuN: 2.005 NO: 1.181 ∠AuNO: 132.4 ∠NAuN: 174.1	1778.3 [9], 1585.2 [4694], 444.4 [1], 416.4 [1], ..., 74.1 [1]
	$^2B_1$ (C_{2v})	+29	0.7500	AuN: 2.093 NO: 1.161 ∠AuNO: 125.6 ∠NAuN: 162.3	1816.9 [138], 1760.5 [2256], 471.2 [23], 442.8 [24], ..., 60.5 [0]
$Au(NO)_2^+$	$^1A'$ (C_{2v})	+763		AuN: 2.275 NO: 1.121 ∠AuNO: 116.2 ∠NAuN: 90.9	2035.5 [698], 1928.3 [1010], 515.3 [25], 482.2 [4], 137.6 [1]

structure, are also associated with the combination band at 3204.1 cm^{-1} (Figure 3). These absorptions show 1:2:1 triplet patterns with $^{14}NO + {}^{15}NO$ (Figure 4), which is reminiscent of the $Cu(NO)_2$ spectrum.[4] The weak 1691.0 cm^{-1} band and matrix site at 1694.8 cm^{-1}, observed only in the mixed isotopic spectrum, are also due to the mixed isotopic product species.

Two additional gold experiments were done to contrast the conditions used for the spectrum in Figure 3: the first employed the same laser energy plus a 10% neutral density filter and the second 3 times the laser energy and no filter, which provides a gold concentration change of more than an order of magnitude.

TABLE 5: Force Constants (N m^{-1}) and Bond Angles (deg) Calculated for AuNO[a]

f_{M-N}		f_{N-O}		$f_{M-N/N-O}$		bond angle	
mean	std dev	mean	std dev	mean	std dev	mean	std dev
294	25	1305	48	95	64	140	10

[a] Argon matrix data.

TABLE 6: Charges Calculated for AuNO and $Au(NO)_2$ Species Using the BPW91 and B3LYP Functionals

molecule (ground state)	BPW91 charges Mulliken/natural			B3LYP charges Mulliken/natural		
	q_{Au}	q_N	q_O	q_{Au}	q_N	q_O
$AuNO^+$ ($^2A'$)	+0.47[a]/+0.74[b]	+0.23/+0.20	+0.30/+0.07	+0.49[a]/+0.75[b]	+0.24/+0.21	+0.27/+0.04
AuNO ($^1A'$)	−0.24/+0.04	+0.08/+0.10	+0.16/−0.14	−0.19/+0.05	+0.06/+0.12	+0.13/−0.17
$Au(NO)_2^+$ ($^1A_1$)	−0.32/+0.52	+0.40/+0.23	+0.25/+0.01	−0.10/+0.54	+0.31/+0.26	+0.24/−0.03
$Au(NO)_2$ (^4B_g)	+0.04/+0.56	−0.03/−0.11	+0.01/−0.17	+0.20/+0.60	−0.09/−0.11	−0.01/−0.19
($^4A_2$)	+0.01/+0.58	−0.03/−0.12	+0.02/−0.17	+0.18/+0.60	−0.08/−0.12	−0.01/−0.18
($^2B_1$)	−0.36/+0.40	+0.14/−0.03	+0.04/−0.17	−0.32/+0.34	+0.13/+0.01	+0.03/−0.18

[a] Mulliken charges. [b] Natural charges.

The relative intensities of the 1710.4 and 1528.2 cm^{-1} bands in these experiments with annealing were approximately the same as in Figure 3. This provides evidence for a common gold stoichiometry and for identification of the 1510.7 and 1528.2 cm^{-1} bands as $Au(NO)_2$ in solid argon and neon. We have no evidence for digold species other than broad bands at 1724 and 1750 cm^{-1} that are favored with high laser power.

Calculations were done for $Au(NO)_2$ using both density functionals, and the trans and cis dinitrosyl quartet state isomers are lower than the cis doublet state with B3LYP but higher with BPW91 (Tables 3 and 4); the trans quartet isomer is 5 kJ/mol lower than cis with both functionals. Although the B3LYP functional usually gives more reliable energies, the energy range (39 kJ/mol) is in accord with the accuracy of these calculations. Both B3LYP and BPW91 quartet state frequency calculations match the observed spectrum very well, and it is likely that both isomers contribute to the observed structured spectrum. A sharp 1528.2 cm^{-1} absorption increases markedly on annealing solid neon to 9 and 11 K but is replaced by a sharp 1532.9 cm^{-1} peak on annealing to 13 K (Figures 3 and 4). It is possible that the 1528.2 cm^{-1} band is due to the $^4A_2$ cis isomer and the 1532.9 cm^{-1} band to the ^4B_g trans isomer with B3LYP calculated frequencies at 1585.2 and 1598.2 cm^{-1}, respectively. In this case the B3LYP frequencies are lower and nearer to the observed values (60 cm^{-1} high) than the BPW91 computations (82 cm^{-1} high). These magnitudes are consistent with the frequency predictions for AuNO although the B3LYP value is higher for AuNO as found for most species.

The combination band at 3204.1 cm^{-1} requires another mode near 3204.1−1528.2 = 1675.9 cm^{-1}, and the quartet states are predicted by B3LYP to have symmetric N−O stretching modes nearly 190 cm^{-1} higher than the antisymmetric modes. The 1691.0 cm^{-1} band is appropriate for the symmetric stretching mode of the $O^{14}N-Au-{}^{15}NO$ isotopic molecule. The 1691.0 cm^{-1} band is 2% of the intensity of the strong 1513.2 cm^{-1} antisymmetric absorption; the BPW91 calculation predicts this symmetric mode to have 3% of the antisymmetric mode intensity for the ^4B_g state and the B3LYP calculation predicts 1%. The sum 1691.0 + 1513.2 = 3204.2 cm^{-1} is 27.7 cm^{-1} above the 3176.5 cm^{-1} combination band observed for the mixed isotopic species. This 27.7 cm^{-1} difference is due to anharmonicity and is near the 32.0 cm^{-1} difference discussed above for AuNO. We deduce the unobserved symmetric stretching mode for $Au(NO)_2$ near 1710 cm^{-1}. The B3LYP frequencies for the ^4B_g state, 1782 and 1598 cm^{-1}, are too high by 72 and 70 cm^{-1}, which is very good agreement for this gold compound. The B3LYP calculation for the AuNO frequency is 114 cm^{-1} higher than the neon matrix frequency.

The $Au(NO)_2$ molecule is observed at 1528.2 cm^{-1}, far below AuNO at 1710.4 cm^{-1} in solid neon. This contrasts $Cu(NO)_2$ at 1635.5 cm^{-1} above CuNO at 1602.2 cm^{-1} and means that the gold−nitrosyl interaction is much stronger in the dinitrosyl than in the mononitrosyl. Although both CuNO and AuNO are $^1A'$ states, $Cu(NO)_2$ appears to be a $^2\Pi_u$ state whereas $Au(NO)_2$ likely has the ^4B_g ground state. The large red-shift of the N−O stretching mode from 1635.5 cm^{-1} for $Cu(NO)_2$ to 1528.2 cm^{-1} for $Au(NO)_2$ indicates that the NO bond lengths are clearly elongated in $Au(NO)_2$ and more electron transfer to NO occurs.

The weaker bands just above $Au(NO)_2$ at 1538.2 and 1556.5 cm^{-1} in solid argon and neon exhibit two intermediate mixed isotopic absorptions in 1:1:1:1 quartet patterns, which indicates two inequivalent NO subgroups. These bands are probably due to a $Au(NO)_2$ species trapped adjacent to another molecule or gold atom where the two NO subunits adopt nonequivalent positions.

A weak band at 1754.5 cm^{-1} in argon increases on annealing, and the ^{15}NO and $^{15}N^{18}O$ counterparts at 1723.8 and 1677.1 cm^{-1} define typical 1.0178 nitrosyl ratios. These bands form asymmetric triplet patterns in both mixed isotopic precursor experiments, but band congestion precludes the possible observation of additional mixed isotopic components. A much weaker feature at 1834.8 cm^{-1} appears to be associated with annealing. These bands are unique to gold experiments and are likely due to gold-perturbed $(NO)_2$.

DFT calculations were done for gold trinitrosyl. A singlet structure failed to converge and a triplet decomposed to $Au(NO)_2$ ($^2B_1$) and NO. However a $^5A''$ state (Table 3) with one shorter and two longer Au−N bonds was 5 kJ/mol more stable than $Au(NO)_2$ (^4B_g) and NO. The strong unique NO frequency predicted at 1619.8 cm^{-1} was not observed in the spectrum although band congestion could preclude the observation of a weak absorption in this region.

$AuNO^+$ and $Au(NO)_2^+$. Sharp, weak bands appear on annealing at 1921.2, 1917.8, 1899.4, 1895.7, and 1892.0 cm^{-1} in solid neon (Figure 5). These bands are 3-fold stronger when the 0.2% NO sample is doped with 0.02% CCl_4 to serve as an electron trap.[13,27] This enhances $(NO)_2^+$ and markedly diminishes $(NO)_2^-$ absorptions as well. In a 1% NO experiment, the latter three absorptions are favored over the former two. The increase in the above absorptions with added CCl_4 relative to AuNO and $Au(NO)_2$ supports their assignment to nitrosyl cations.[13] A similar enhancement was observed for $Au(CO)_n^+$ absorptions in the carbon monoxide investigation.[27] Matching ^{15}NO counterparts (Table 2) were observed in a CCl_4-doped ^{15}NO experiment, but the region was too congested to observe mixed isotopic counterparts. The 1921.2 and 1917.8 cm^{-1} bands are assigned to $AuNO^+$ and the 1899.4, 1895.7, and 1892.0 cm^{-1} bands to $Au(NO)_2^+$ in different matrix sites. DFT calculations for $AuNO^+$ give frequencies in very good agreement with experiment. Both functionals predict a $^2A'$ ground state, with nitrosyl stretching frequencies 1935.4 cm^{-1} (BPW91) and 2015.4 cm^{-1} (B3LYP). The former is only 14−17 cm^{-1} higher than the experimental value, similar to the 54 cm^{-1} difference between theory and experiment for AuNO, and the latter requires a scale factor of 0.95 to agree with experiment, similar to the factor 0.94 for AuNO. Both functionals predict a very strong

antisymmetric N−O fundamental for the dinitrosyl cation slightly below the mononitrosyl cation in good agreement with the observed matrix-site absorptions. The weaker symmetric mode was not observed.

Cationic gold complexes have been characterized for a number of small ligands.[28] A particularly interesting comparison can be made between $AuNO^+$ and $AuCO^+$ as both have been observed in solid neon: the blue shifts in ligand stretching modes relative to the isolated ligand in solid neon are 43.4 and 96.0 cm^{-1}, respectively.[13] The B3LYP calculated ligand binding energies are 32 and 44 kcal/mol for $AuNO^+$ and $AuCO^+$, respectively.[28] The Au^+ interaction with NO is clearly weaker than with CO.

Comparisons with Zeolite Spectra. The matrix spectra provide reference points for comparison of NO species adsorbed on zeolites. The N−O absorptions on zeolites[2,3] ranging between 1910 and 1740 cm^{-1} are best ascribed to mononitrosyl species with decreasing positive charge. On the basis of the present calculations and observations, gold dinitrosyl species should absorb between 1900 and 1500 cm^{-1}, again depending on the positive charge. The 1837 and 1741 cm^{-1} bands ascribed[3] to $Au^I(NO)_2$, if indeed due to a dinitrosyl, require a metal center with a fractional positive charge.

Bonding in AuNO Species. The bonding in AuNO and $AuNO^+$ has been examined using the molecular orbitals and natural bond orbitals (NBO).[29] The bonding in $AuNO^+$ is found to be completely analogous to that for $AgNO^+$ and $CuNO^+$ as described previously with both functionals.[4,5,30] The uppermost occupied orbital is formed primarily from the Au(6s) orbital and the in-plane NO($2\pi^*$) molecular orbital and is bonding between the Au and N atoms but antibonding between the N and O atoms. The next lowest orbitals are formed almost exclusively from the Au(5d) orbitals and do not mix significantly with orbitals on NO. The NBO analysis for $AuNO^+$ shows a one-electron bond between gold and nitrogen that is 34% Au (86% 6s, 14% 5d) and 66% N (3% 2s, 97% 2p) (BPW91). This is qualitatively similar to that in $AgNO^+$, which is 15% Ag (97% 5s, 2% 5p, 17% 4d) and 85% N (2% 2s, 98% 2p),[5] and $CuNO^+$, which is 12% Cu (93% 4s, 3% 4p, 4% 3d) and 88% N (9% 2s, 91% 2p),[30] but there are two significant differences. The first is that the participation by the gold orbitals is more than double that of silver in $AgNO^+$, and the second is the greater sd hybridization on gold compared to silver, where the Ag(5s) orbital comprises 97% of the metal contribution to the natural orbital. The latter can be attributed to the smaller energy difference between the *n*s and $(n-1)$d orbitals in gold compared to silver, which arises due to the stronger relativistic effect in the third transition row.[31,32] The former is also due to the lower energy of the Au(6s) orbital than the Ag(5s) orbital, lower than the energy of the NO $2\pi^*$ orbital as calculated by DFT. The NBO analysis also shows the NO bond order to be 2.5, composed of a σ bond, an out-of-plane π bond, and a singly occupied in-plane π bond. The HOMO in $AuNO^+$ may be described as a one-electron dative bond between the gold and nitrogen atoms. This partial electron donation from the NO molecule decreases the positive charge on gold, as shown by the Mulliken and natural charges (Table 6). This decrease in electron density from the antibonding orbital explains the high 1935.4 cm^{-1} frequency and the short 1.130 Å N−O bond length calculated for $AuNO^+$. This frequency is still way short of NO^+ at 2343.9 cm^{-1} in the gas phase.[17]

The molecular orbitals for AuNO are essentially the same as those in $AuNO^+$ except that the HOMO is doubly occupied. This increases the Au−N bond order but decreases the N−O bond order, as shown by the shorter Au−N bond and longer N−O bond calculated in AuNO relative to $AuNO^+$. The NBO analysis gives the same picture for AuNO, describing the Au−N and N−O linkages as single and double bonds, respectively. The natural orbital between gold and nitrogen is composed of 47% Au (77% 6s, 23% 5d) and 53% N (3% 2s, 97% 2p) orbitals (BPW91); the increased participation of gold arises from the Au(6s) electron to form a two electron covalent bond. This bond is essentially unpolarized, unlike the equivalent orbital in neutral $AgNO^+$, which is 36% Ag (95s, 5% 4d) and 64% N (100% 2p) (BPW91) where more charge transfer takes place. We believe the natural charges are more realistic for AuNO as the 1701.9 cm^{-1} frequency is 170 cm^{-1} below that for NO, and the NO subunit contains a small negative charge (Table 6). This negative charge increases to −0.16 for AgNO and to −0.25 for CuNO as the frequency decreases to 1680.3 and 1587.1 cm^{-1}, respectively, in solid argon.[4,5]

The comparison between AuNO and $Au(NO)_2$ is of interest as the average dinitrosyl frequency is much less than the mononitrosyl mode, which is opposite that found for late first-row TM nitrosyls[13] and particularly copper[4] where both $Cu(NO)_2$ fundamentals are above the CuNO value. This indicates a stronger gold bonding interaction when bound to two NO subunits than with a single NO. The natural orbital between gold and nitrogen for the ^4B_g state is composed of 22% Au (76% 6s, 24% 5d) and 78% N (20% 2s, 80% 2p) (BPW91) (the B3LYP results and $^4A_2$ state are essentially the same). Although gold is now bonding to two nitrosyls, the 22% Au character is slightly less than half of the 47% Au character for AuNO. The Au−NO bond length is much longer (2.094 Å/BPW91) and the Au−N−O angle is smaller (118.8°/BPW91), which result from the strong interaction of the 5σ MO of NO and the d_σ orbital of Au in AuNO. However, the Au−N−O angle increases to 134.5° in $Au(NO)_2$, which shows that the strong σ interaction is partly eliminated through sd hybridization and charge transfer. The NBO population analysis (Table 6) shows that much more charge transfer occurs in $Au(NO)_2$ than in AuNO. The net positive charge on Au in $Au(NO)_2$ is 0.56 (BPW91) and 0.60 (B3LYP), respectively, which are much larger than on Au in AuNO, and even larger than on Au in $Au(NO)_2^+$. Accordingly, NO in $Au(NO)_2$ gains more negative charge. As a result, the NO bond elongates and the NO stretching vibration is lower by about 100 cm^{-1}. It is interesting to note that the Au−N−O angles in both $AuNO^+$ and $Au(NO)_2^+$ are very close (Tables 3 and 4), which is indicative of nearly the same σ interaction for the two cations and therefore the NO stretching vibrations are close to each other.

Conclusions

Laser-ablated gold reacts with nitric oxide to form the nitrosyl products AuNO and $Au(NO)_2$. The relative frequencies for AuNO and $Au(NO)_2$ are reversed from those for the analogous copper nitrosyls: the gold interaction is stronger in the dinitrosyl, sd hybridization is more extensive, and more charge-transfer occurs. The DFT calculations are reasonably effective in reproducing the experimental frequencies, but both BPW91 and B3LYP functionals consistently overestimate the vibrational frequencies, by 60−110 cm^{-1}, requiring scale factors near 0.94 to agree with experiment. This is a greater error than was found with the lighter Cu and Ag metal nitrosyls, but the calculations for Au nitrosyls do give chemically useful results. Consistent with increased sd hybridization, the computed AuNO angle increases about 15° in $Au(NO)_2$ compared to AuNO. A natural orbital analysis shows greater participation of gold 5d orbitals

than silver 4d in bonding to NO. The BPW91 calculation predicts that AuNO is bound by 117 kJ/mol, but a second NO is bound by 42 kJ/mol. Finally, sharp, weak bands enhanced by CCl_4 added as an electron trap are assigned to $AuNO^+$ and $Au(NO)_2^+$.

Acknowledgment. We gratefully acknowledge financial support from NSF Grant CHE 00-78836.

References and Notes

(1) Galvagno, S.; Parravano, G. *J. Catal.* **1978**, *55*, 178.
(2) Salama, T. M.; Ohnishi, R.; Shido, T.; Ichikawa, M. *J. Catal.* **1996**, *162*, 169.
(3) Qiu, S.; Ohnishi, R.; Ichikawa, M. *J. Phys. Chem.* **1994**, *98*, 2719.
(4) Zhou, M. F.; Andrews, L. *J. Phys. Chem. A* **2000**, *104*, 2618 (Cu + NO).
(5) Citra, A.; Andrews, L. *J. Phys. Chem A* **2001**, *105*, 3042 (Ag + NO).
(6) Burkholder, T. R.; Andrews, L. *J. Chem. Phys.* **1991**, *95*, 8697. Hassanzadeh, P.; Andrews, L. *J. Phys. Chem.* **1992**, *96*, 9177.
(7) Frisch, M. J.; Trucks, G. W.; Schlegel, H. B.; Gill, P. M. W.; Johnson, B. G.; Robb, M. A.; Cheeseman, J. R.; Keith, T.; Petersson, G. A.; Montgomery, J. A.; Raghavachari, K.; Al-Laham, M. A.; Zakrzewski, V. G.; Ortiz, J. V.; Foresman, J. B.; Cioslowski, J.; Stefanov, B. B.; Nanayakkara, A.; Challacombe, M.; Peng, C. Y.; Ayala, P. Y.; Chen, W.; Wong, M. W.; Andres, J. L.; Replogle, E. S.; Gomperts, R.; Martin, R. L.; Fox, D. J.; Binkley, J. S.; Defrees, D. J.; Baker, J.; Stewart, J. P.; Head-Gordon, M.; Gonzalez, C.; Pople, J. A. *Gaussian 94*, revision B.1; Gaussian, Inc.: Pittsburgh, PA, 1995.
(8) Becke, A. D. *Phys. Rev. A* **1988**, *38*, 3098.
(9) Perdew, J. P.; Wang, Y. *Phys. Rev. B* **1992**, *45*, 13244.
(10) Becke, A. D. *J. Chem. Phys.* **1993**, *98*, 5648.
(11) Krishnan, R.; Binkley, J. S.; Seeger, R.; Pople, J. A. *J. Chem. Phys.* **1980**, *72*, 650.
(12) Wadt, W. R.; Hay, P. J. *J. Chem. Phys.* **1985**, *82*, 284. Hay, P. J.; Wadt, W. R. *J. Chem. Phys.* **1985**, *82*, 299.
(13) Zhou, M. F.; Andrews, L. *J. Phys. Chem. A* **2000**, *104*, 3915 (Ni + NO) and references therein.
(14) Andrews, L.; Zhou, M. F.; Willson, S. P.; Kushto, G. P.; Snis, A.; Panas, I. *J. Chem. Phys.* **1998**, *109*, 177 (NO in argon) and references therein.
(15) Andrews, L.; Zhou, M. F. *J. Chem. Phys.* **1999**, *111*, 6036 (NO in neon) and references therein.
(16) Lugez, C. L.; Thompson, W. E.; Jacox, M. E.; Snis, A.; Panis, I. *J. Chem. Phys.* **1999**, *110*, 10345.
(17) Citra, A.; Andrews, L. *J. Phys. Chem. A* **2000**, *104*, 8689 (Os, Ru + NO).
(18) Citra, A.; Andrews, L. *J. Phys. Chem. A* **2000**, *104*, 11897 (Rh, Ir + NO).
(19) Citra, A.; Andrews, L. *J. Phys. Chem. A* **2000**, *104*, 8160 (Pd, Pt + NO).
(20) Zhou, M. F.; Andrews, L. *J. Phys. Chem. A* **1998**, *102*, 7452 (Cr + NO).
(21) Andrews, L.; Zhou, M. F.; Ball, D. W. *J. Phys. Chem. A* **1998**, *102*, 10041 (Mn + NO).
(22) Zhou, M. F.; Andrews, L. *J. Phys. Chem. A* **1999**, *103*, 478 (V + NO).
(23) Kushto, G. P.; Zhou, M. F.; Andrews, L.; Bauschlicher, C. W., Jr. *J. Phys. Chem. A* **1999**, *103*, 1115 (Sc, Ti + NO).
(24) Zhou, M. F.; Andrews, L. *J. Phys. Chem. A* **1998**, *102*, 10025 (Nb, Ta + NO).
(25) Andrews, L.; Zhou, M. F *J. Phys. Chem. A* **1999**, *103*, 4167 (Mo + NO).
(26) Huber, H.; Herzberg, G. *Constants of Diatomic Molecules*; Van Nostrand: New York, 1979.
(27) Liang, B.; Andrews, L. *J. Phys. Chem. A* **2000**, *104*, 9156.
(28) Schröder, D.; Schwarz, H.; Hrušák, J.; Pyykkö, P. *Inorg. Chem.* **1998**, *37*, 624 and references therein.
(29) Reed, A. E.; Curtiss, L. A.; Weinhold, F. *Chem. Rev.* **1988**, *88*, 899.
(30) Thomas, J. L. C.; Bauschlicher, C. W., Jr.; Hall, M. B. *J. Phys. Chem. A* **1997**, *101*, 8530.
(31) Pyykkö, P. *Chem. Rev.* **1988**, *88*, 56**.**
(32) Schwerdtfeger, P.; Bowmaker, G. A. *J. Chem. Phys.* **1994**, *100*, 4487.